Electronic Supplementary Information (ESI) for

Schiff base organic molecular crystals/ferroelectric polymer composite for photo-pyroelectric conversion

Zhaopeng Wang [a], Jie Liu [a] and Baojin Chu [a, *]

[a] CAS Key Laboratory of Materials for Energy Conversion and Department of Materials Science and Engineering, University of Science and Technology of China, Hefei, Anhui Province, 230026, China

Zhaopeng Wang: wangzp1@mail.ustc.edu.cn

Jie Liu: lj626@ustc.edu.cn

* Corresponding author. Baojin Chu: chubj@ustc.edu.cn

This PDF file includes:

Supporting text

Figures S1 to S7

Table S1

Legends for Movies S1 to S2

SI References

S1. Experimental Section

Materials

2-Hydroxy-1-naphthaldehyde and 4-nitro-1-naphthylamine were purchased from Aladdin Industrial Corporation, China. P(VDF-TrFE) (65/35) was purchased from Piezotech, Arkema Group, France. *N*, *N*-Dimethylformamide (DMF) was purchased from Sinopharm Chemical Reagent Co., Ltd., China. All the materials were used as received without any further treatment.

A liquid crystal display (LCD, EDS812) was purchased from Dalian Qiyun Display Co., Ltd., China. Capacitors were purchased from Dongguan Chengxing Electronic Co., Ltd., China. An electrochromic display (ECD) device was purchased from Zhuhai Kaivo Optoelectronic Technology Co., Ltd., China.

Synthesis of HNAN-NO_2

Synthesis of 2-hydroxynaphthylidene-4'-nitro-1'-naphthylamine (HNAN-NO_2)[1] (Fig. S1): A solution of 2-hydroxyl-1-naphthaldehyde (2.5 mmol) and 4-nitro-1-naphthylamine (2.5 mmol) in ethanol (40 mL) was heated to 75 °C for 5 hours. A red precipitate was obtained by filtering and repeatedly washing the reaction product with alcohol. ^{1}H NMR (600 MHz, DMSO-d_6, δ) is shown in Fig. S1: 15.08 (d, J = 2.4 Hz, 1H), 9.82 (d, J = 2.5 Hz, 1H), 8.64 (d, J = 8.3 Hz, 1H), 8.51 (d, J = 8.7 Hz, 1H), 8.45 (d, J = 8.2 Hz, 1H), 8.37 (d, J = 8.6 Hz, 1H), 8.06 (d, J = 9.3 Hz, 1H), 7.86 (dd, J = 8.2, 5.0 Hz, 3H), 7.82 (d, J = 7.7 Hz, 1H), 7.59 (s, 1H), 7.41 (d, J = 7.5 Hz, 1H), 7.19 (d, J = 9.2 Hz, 1H).

Fabrication of composite films

Composite films of the P(VDF-TrFE) copolymer with HNAN-NO_2 were prepared by a solution casting method (Figure S3). Schiff base compounds and P(VDF-TrFE) were first dissolved in DMF and stirred overnight. The homogenous mixture was subsequently cast on a clean glass plate and dried in an oven at 80 °C for 2 h. After cooling to room temperature naturally, the composite films were peeled off from the glass plate and dried in a vacuum oven at 135 °C for 5 h to remove residual solvent and improve crystallinity. The thickness of the films was approximately 20 μm.

Characterization

The ultraviolet-visible (UV–Vis) spectra were recorded on a spectrophotometer (SOLID3700, Shimadzu, Japan). The morphology and microstructure of the HNAN-NO_2 crystals and composite films were examined by a scanning electron microscopy (SEM, SU8220, HITACHI, Japan), a transmission electron microscopy (TEM, JEM F200, JEOL, Japan), a Nicolet 8700 FT–IR spectrometer (Thermo Nicolet, USA), and a multifunctional rotating-anode X-ray diffractometer (SmartLab, Rigaku, Japan) with Cu Kα radiation. The phase transition temperature and enthalpy were measured by a differential scanning calorimeter (DSC 214 Polyma, NETZSCH, Germany) at a heating rate of 5 °C min^{-1} under a nitrogen atmosphere. The mechanical properties of the copolymer and composite films were measured by a dynamic mechanical analyzer (DMA Q800, TA Instruments, USA) at a strain rate of 100 μm/min. The temperature of the HNAN-NO_2 crystal aqueous dispersion and composite films

under light illumination was captured by an infrared camera (ImageIR 8325, InfraTec, Germany).

To measure the electrical properties of the composite films, gold electrodes (~40 nm) or ITO electrodes (~100 nm) were coated on both sides of the films by a sputter coater (LAB 18, Kurt J. Lesker, USA). The temperature and frequency dependence of the dielectric properties of the films were measured using an automated measurement system composed of a furnace and an LCR meter (E4980, Agilent Technology, USA). The polarization versus electric field curves (*P–E* loops) were measured using a modified Sawyer-Tower circuit (Polyktech, State College, USA). The films used in the photo-electric response test were polarized using a DC-regulated power supply (CS2671B, Nanjing Changsheng Instrument Co., Ltd., China) at an electric field of 100 MV m^{-1} for 5 min. The open-circuit voltage, short-circuit current, and thermally stimulated depolarization current curve of the composite film were measured by an electrometer (Keithley 6517A, Tektronix Inc., USA).

S2. Calculation of the current values of the pyroelectric response

According to pyroelectric theory, the pyroelectric current can be given by:[2]

$$i = pA\frac{dT}{dt}$$

where p is the pyroelectric coefficient, A is the electrode area, and dT/dt is the temperature change rate.

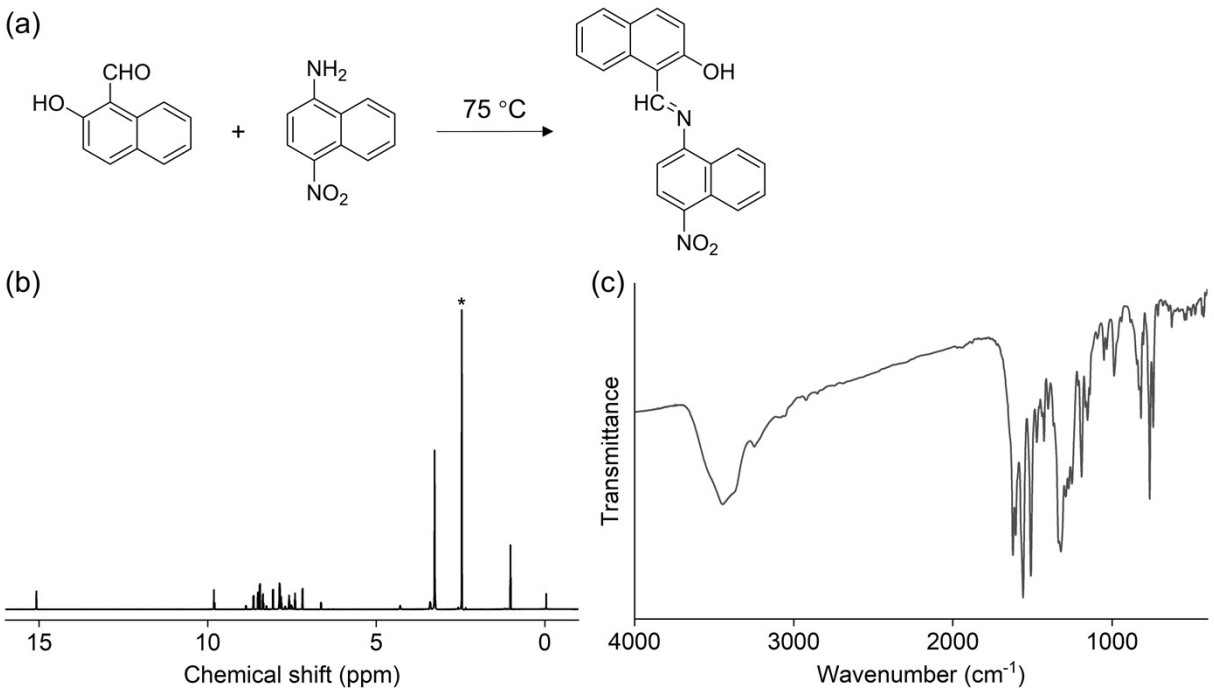

Figure S1. a) Chemical reaction of HNAN-NO_2. b) ^{1}H-NMR spectra, and c) FT-IR spectra of HNAN-NO_2.

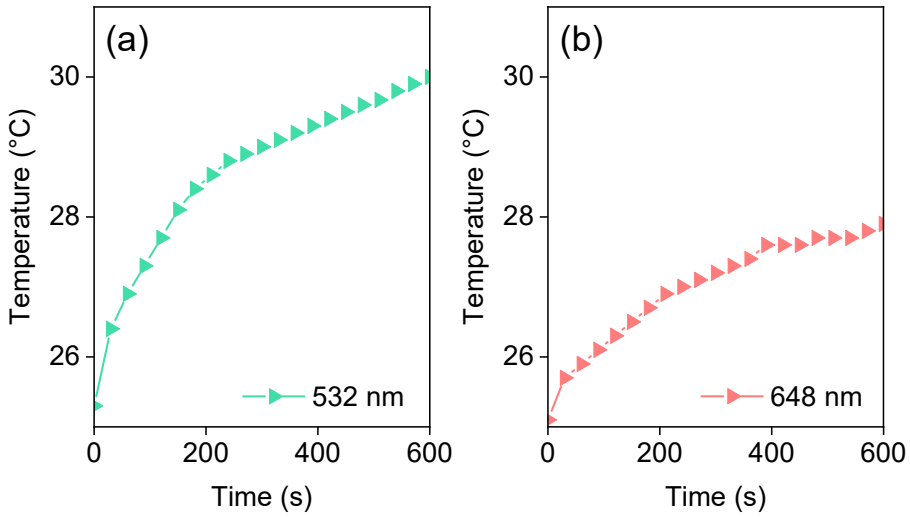

Figure S2. Photothermal heating curve of the HNAN-NO_2 molecular crystal dispersion (500 μg mL^{-1} aqueous dispersion) under irradiation with a) 532 nm and b) 648 nm light sources (power density: 300 mW cm^{-2}).

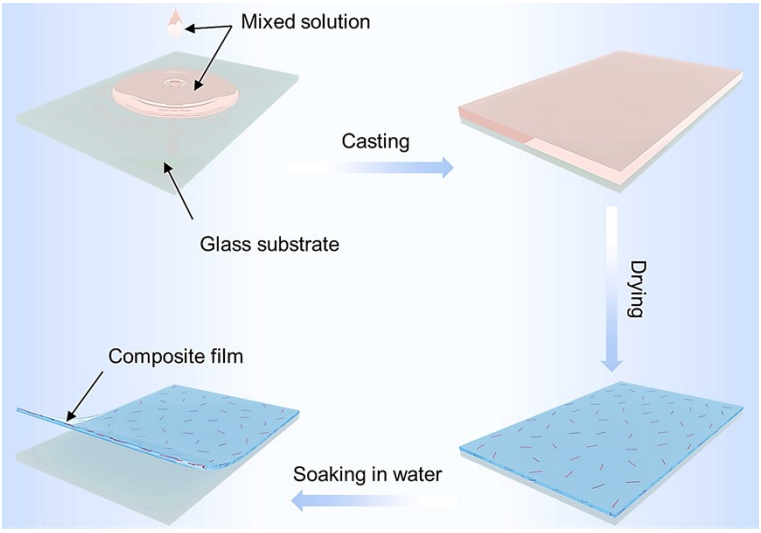

Figure S3. Schematic diagram of the fabrication process of the composite films.

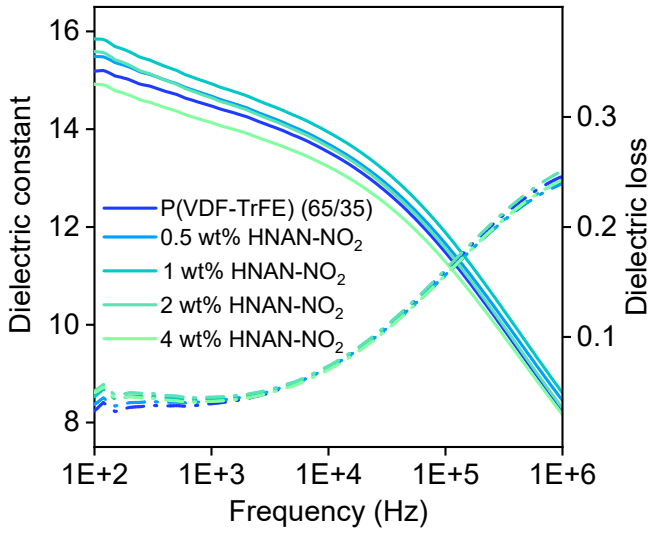

Figure S4. Frequency-dependent dielectric constant and loss of the P(VDF-TrFE) copolymer and composite films containing 0.5-4 wt% HNAN-NO_2.

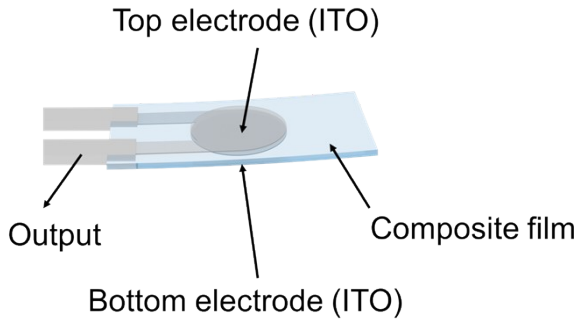

Figure S5. Schematic diagram of the samples used for the photo-electric conversion test. The electrodes are composed of two round transparent ITO electrodes with tails on the upper surface and the lower surface of the film to minimize the effect of the electrode material on the light absorption of the tested films. The overlapping circular electrode area in the middle receives light as the test area (the effective area for pyroelectric calculations). The two tails on the same sides of the upper and lower surfaces are used for electrical connections.

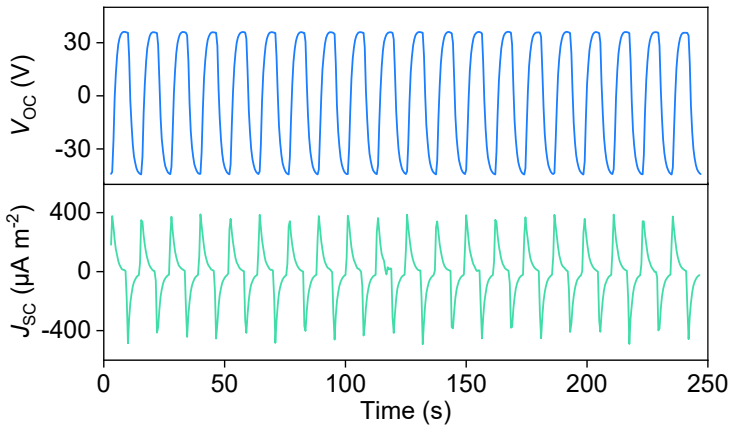

Figure S6. Open-circuit voltage (V_{OC}) and short-circuit current density (J_{SC}) output versus time curves for a composite film that was repeatedly bent 50 times (light wavelength: 450 nm, power density: 100 mW cm^{-2}, frequency: 83.3 mHz).

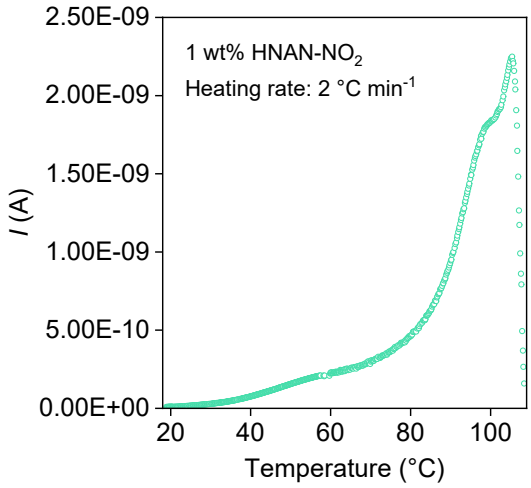

Figure S7. Thermally stimulated depolarization current curve of the 1 wt% HNAN-NO_2 composite film.

Table S1. Performance comparison between this work and previous reports on photo-electric conversion materials based on ferroelectric polymers.

Composite	Light source /mW cm^{-2}	Temperature change /°C	V_{OC} /V	I_{CD} /μA m^{-2}	E_{OC} /MV m^{-1}	Ref.
Graphene/PVDF/Graphene	IR Lamp: 2000	38	2	500	0.01	3
Graphene ink/PVDF	IR Lamp: 340	5	24	35	0.46	4
PVDF/$WO_{2.72}$	IR Lamp: 226	92.6	1.5	27.8	N/A	5
PEDOT/PVDF/PEDOT	IR Lamp: 1450	4	4	75	0.13	6
Graphene–PDMS/PVDF	IR Lamp: 160	78.3	20	50	N/A	7
LMPs/P(VDF-TrFE)	IR Lamp: 42	~11	~20	~150	~0.18	8
$BiFeO_3$–$BaTiO_3$/P(VDF-TrFE)	IR Lamp: 27	~11	8	N/A	~0.4	9
F-Azo@AG/PVDF	Solar Lamp: 100	3	0.164	N/A	~0.006	10
TiO_2/Cu-SiO_2/PVDF	Solar Lamp: 100	15.9	8.2	4.4	N/A	11
rGO-PEI/PVDF	Solar Lamp: 100	60.8	-93.1	-229	1.75	12
azoBPA-6FDI/PVDF	445 nm Lamp: 120	N/A	0.006	N/A	0.00075	13
LLCP/P(VDF-TrFE)	470 nm Lamp: 80	2.2	0.79	67	0.395	14
HNAN-NO_2/P(VDF-TrFE)	450 nm Lamp: 100	18	36.6	439.4	1.83	This work

Since the electric voltage values resulting from piezoelectric and pyroelectric effects are dependent on sample dimensions, we converted the V_{OC} into an electric field (E_{OC}) for comparison with the results of other different works.

Supplementary Videos

Video S1. A demonstration video showing that a photo-pyroelectric composite film supplies power to a liquid crystal display (LCD) screen placed in a vacuum chamber under 450 nm light illumination.

Video S2. A demonstration video showing an electrochromic display (ECD) device driven by a system consisting of a photo-pyroelectric composite film and a capacitor.

SI References

1. Z. P. Wang, J. Liu, K. W. Yi, P. Chen, Y. H. Zhu, D. X. Tian and B. J. Chu, *Chemical Engineering Journal*, 2023, **455**, 140693.
2. C. R. Bowen, J. Taylor, E. LeBoulbar, D. Zabek, A. Chauhan and R. Vaish, *Energy Environ. Sci.*, 2014, **7**, 3836-3856.
3. H. Z. Liu, T. T. Zhao, W. T. Jiang, R. Jia, D. Niu, G. L. Qiu, L. Fan, X. Li, W. H. Liu, B. D. Chen, Y. S. Shi, L. Yin and B. H. Lu, *Adv. Funct. Mater.*, 2015, **25**, 7071-7079.
4. D. Zabek, K. Seunarine, C. Spacie and C. Bowen, *ACS Appl. Mater. Interfaces*, 2017, **9**, 9161-9167.
5. C. M. Wu, M. H. Chou, T. F. Chala, Y. Shimamura and R. Murakami, *Compos. Sci. Technol.*, 2019, **178**, 26-32.
6. W. T. Jiang, T. T. Zhao, H. Z. Liu, R. Jia, D. Niu, B. D. Chen, Y. S. Shi, L. Yin and B. H. Lu, *RSC Adv.*, 2018, **8**, 15134-15140.
7. W. Y. Wei, J. J. Gao, J. F. Yang, J. Wei and J. B. Guo, *RSC Adv.*, 2018, **8**, 40856-40865.
8. F. Wang, M. J. Liu, C. Liu, C. Huang, L. D. Zhang, A. Y. Cui, Z. G. Hu and X. M. Du, *Natl. Sci. Rev.*, 2023, **10**, 9.
9. X. P. Hu, Y. P. Che, Z. J. Zhang, Q. D. Shen and B. J. Chu, *ACS Appl. Electron. Mater.*, 2021, **3**, 743-751.
10. Y. B. Xiong, L. D. Zhang, P. Weis, P. Naumov and S. Wu, *J. Mater. Chem. A*, 2018, **6**, 3361-3366.
11. X. Q. Wang, C. F. Tan, K. H. Chan, K. C. Xu, M. H. Hong, S. W. Kim and G. W. Ho,

ACS Nano, 2017, **11**, 10568-10574.

12. H. T. Li, C. S. L. Koh, Y. H. Lee, Y. H. Zhang, G. C. Phan-Quang, C. Zhu, Z. Liu, Z. S. Chen, H. Y. F. Sim, C. L. Lay, Q. An and X. Y. Ling, *Nano Energy*, 2020, **73**, 104723.

13. J. J. Wie, D. H. Wang, V. P. Tondiglia, N. V. Tabiryan, R. O. Vergara-Toloza, L. S. Tan and T. J. White, *Macromol. Rapid Commun.*, 2014, **35**, 2050-2056.

14. B. Peng, X. Chen, G. Yu, F. Xu, R. Yang, Z. Yu, J. Wei, G. Zhu, L. Qin, J. Zhang, Q. Shen and Y. Yu, *Adv. Funct. Mater.*, 2023, **33**, 2214172.